
Quantum Phase Transition of the Spin-1-Boson Model

Quantenphasenübergang des Spin-Boson Modells mit Spin 1

Bachelorarbeit
an der Ludwig-Maximilians-Universität
München

vorgelegt von
Manuel Lindner
aus München



Gutachter Prof. Dr. Jan von Delft
München, den 30. Juni 2014

Contents

1	Introduction	4
2	Phase Transitions	6
2.1	Classical and Quantum Phase Transitions	6
2.2	Critical Exponents	7
2.3	Mean-Field Theories	8
2.4	Quantum-to-Classical Correspondence	9
3	The Spin-Boson Model	10
3.1	The Hamiltonian	10
3.2	Critical Behaviour	11
3.3	Spin-1-Boson Model	13
4	Numerical Methods	14
4.1	Discretization and Mapping of the Hamiltonian	14
4.2	NRG Procedure	15
4.2.1	Shortcomings of Bosonic NRG	16
4.3	VMPS Approach	16
4.3.1	Matrix Product States	17
4.3.2	Variational Optimization	17
4.3.3	Capture of the Bosonic Shifts	18
5	Results	19
5.1	Phase Boundary	19
5.2	Critical Exponents	21
6	Conclusion	26
7	Appendix	27
7.1	Derivation of the Spin-1 Matrices	27
	Bibliography	29

1 Introduction

The Spin-Boson Model has attracted lots of attention within condensed matter theory in recent years. As the simplest type of bosonic quantum impurity models it paved the way to a deeper understanding of dissipation in quantum systems. Since the publication of Leggett et al. in 1987 [1], many aspects of the model have been studied including its quantum phase transition at zero temperature. A key factor for these studies has been the development of powerful numerical methods, which allowed gaining new insights into critical behaviour. The most prominent technique is the Numerical Renormalization Group (NRG), developed in the 1970s by Kenneth Wilson [2]. Originally applied to solve the Kondo problem [3], NRG nowadays represents the most powerful approach towards fermionic quantum impurity models.

For over three decades, the application of NRG was restricted to fermionic models. The underlying reason for this restriction lies in Pauli's exclusion principle: in fermionic systems each state can be occupied at most once, whereas in bosonic systems the occupation of a state can be arbitrary high. This leads to an infinitely large Hilbert space in the bosonic case that is hard to treat numerically and requires a systematic truncation scheme. Therefore it took until 2003 to introduce a bosonic NRG scheme for the application to the Spin-Boson Model [4].

The resulting data for the Spin-Boson Model soon led to much controversy regarding its quantum phase transition: theoretical considerations based on quantum-to-classical correspondence (QCC) yielded values for critical exponents that were inconsistent with the NRG calculations. This resulted in the striking conclusion that QCC would fail for the Spin-Boson Model [5].

However, the authors of [5] concluded afterwards that in fact the NRG results were incorrect due to the bosonic state space truncation [6]. At the same time, other methods like Quantum Monte Carlo [7] and exact diagonalization [8] confirmed the QCC predictions. In order to fix the bosonic truncation error, a Variational Matrix Product State (VMPS) approach has been introduced by Guo et al. [9]. Although it is partly based on NRG, it deals with the truncation problem in a much more systematic way leading to results in excellent agreement with QCC. Therefore it can be concluded without much doubt that QCC is valid for the Spin-Boson Model.

In this thesis, the VMPS method is used to study a slightly modified version of the standard Spin-Boson Model by using an impurity spin 1, in contrast to the standard spin $1/2$.

The thesis is organized as follows:

- Chapter 2 gives a short outline about the theory of phase transitions with the focus

on the features that are relevant for this thesis.

- Chapter 3 reviews the important physical aspects of the Spin-Boson Model.
- Chapter 4 summarizes the numerical methods that are used in this thesis for the study of the Spin-Boson Model.
- Chapter 5 presents the results for the Spin-1-Boson Model.

2 Phase Transitions

This chapter summarizes the essential features of the physics of phase transitions. We focus only on aspects that are significant for the study of the Spin-Boson Model.

For a more elaborate discussion on this topic see [10].

2.1 Classical and Quantum Phase Transitions

Phase transitions are a ubiquitous phenomenon in physics. Common examples are the transition from water to ice at zero degree temperature, the transition from ferromagnetism to paramagnetism at the Curie temperature or the change between crystalline structures.

Such phenomena can be explained by considering the free energy $F = U - TS$. Per definition, a system is in thermal equilibrium when its free energy is minimized. F consists of two competing terms: the internal energy U that is usually minimized for an ordered system (e.g. for equally aligned magnetic moments in a ferromagnet) and the second term with the entropy S , which prefers disorder. By tuning the temperature T over a critical value T_c (the Curie temperature in the case of ferromagnets), one can therefore qualitatively change the properties of the system. That kind of behaviour is distinctive for a phase transition.

Of particular interest are second-order or continuous phase transitions. Here, the free energy F is continuous in its first derivative and has a discontinuity in its second derivative at the critical point, in contrast to first-order phase transitions which exhibit a discontinuity in the first derivative of F .

As an example for a continuous phase transition, consider again the case of ferromagnets: for $T > T_c$ thermal fluctuations destroy any magnetic order of the system. Hence, the magnetic moments are completely uncorrelated (see Figure 2.1). Approaching T_c from above, areas of same magnetization are formed and the correlations become long ranged. Below the critical point T_c all magnets either point up or down. The system has a finite magnetization m and the correlation length ξ diverges, which is a distinctive feature of second-order phase transitions.

For a mathematical description of this behaviour, one introduces the order parameter m , which measures the degree of order in the system. It is always zero in the disordered phase ($T > T_c$) and finite in the ordered phase ($T < T_c$). In the case of ferromagnets, the order parameter is the magnetization. For second-order phase transitions, the order parameter vanishes continuously near the critical point coming from the ordered phase with $m \propto |T - T_c|^\beta$, where β is a critical exponent defined in the next section.

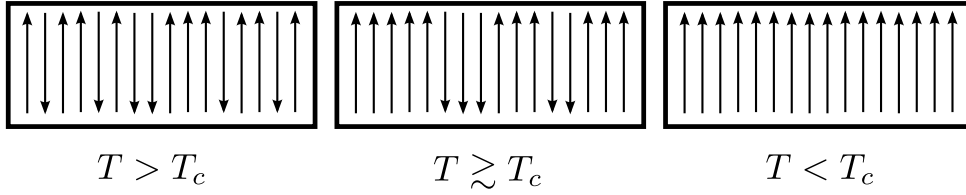


Figure 2.1: Simplified model of a ferromagnet. In the disordered phase ($T > T_c$) the magnetic moments are uncorrelated, whereas in the ordered phase they are fully correlated leading to magnetization.

Considering the above mentioned examples, one would expect phase transitions to occur only for finite temperature $T > 0$. However, there exists another interesting class of phase transitions, so called quantum phase transitions, which have been intensively studied in the last decades [11][10][12]. Occuring at $T = 0$, the source driving these transitions can not be thermal fluctuations. Instead, quantum fluctuations resulting from Heisenberg's uncertainty principle are responsible for this type of transition. The tunable parameter controlling the transition must be non-thermal and could for example be a coupling strength. Although these transitions only appear at $T = 0$, they strongly influence the finite temperature phase diagram of certain materials. Hence, quantum phase transitions open up a new field of research with applications ranging from the study of qubits [13] to superconducting materials [14].

2.2 Critical Exponents

The behaviour of a system at criticality can be quantified by its critical exponents that describe the characteristic scaling of physical observables close to the critical point. In the last section, we have already encountered one example of a critical exponent, namely the order parameter exponent β . For magnetic systems, the common critical exponents are summarized in Table 2.1.

Physical Observable	Exponent	Definition	Conditions
specific heat	α	$C \propto t ^{-\alpha}$	$t \rightarrow 0, B = 0$
order parameter	β	$m \propto t ^\beta$	$t \rightarrow 0^-, B = 0$
susceptibility	γ	$\chi \propto t ^{-\gamma}$	$t \rightarrow 0, B = 0$
magnetic field	δ	$B \propto m ^\delta \text{sgn}(m)$	$t = 0, B \rightarrow 0$
correlation length	ν	$\xi \propto t ^{-\nu}$	$t \rightarrow 0, B = 0$
correlation function	η	$G(r) \propto r ^{-d+2-\eta}$	$t = 0, B = 0$
correlation time	z	$\tau_c \propto \xi^z$	$t \rightarrow 0, B = 0$

Table 2.1: Common critical exponents for magnetic (Ising-like) models with an external magnetic field B . t is the dimensionless distance from criticality, $t = \frac{T-T_c}{T_c}$. $G(r)$ is the correlation function of two spins with distance r and τ_c is the correlation time. Adapted from [12].

As we elaborate on in the next section, critical exponents have a high degree of universality, i.e. they can take the same values for a whole class of systems, independent of their microscopic details.

2.3 Mean-Field Theories

Mean-field theories are a very important concept in order to study phase transitions. The idea is to replace the many-body interaction terms in the Hamiltonian by a one-body interaction. In this approximation, the partition function can often be calculated analytically and the critical exponents can be extracted. The such obtained critical exponents are found to be universal for all classical systems and take the values listed in Table 2.2.

Exponent	Value
α	0
β	1/2
γ	1
δ	3
ν	1/2
η	0

Table 2.2: Values for the critical exponents of classical systems in the mean-field approximation. Adapted from [12].

However, mean-field theories have severe limitations, since they do not take fluctuations of the physical quantities into account. As these fluctuations play a crucial role in the vicinity of the critical point, the mean-field predictions for critical exponents are only valid if their effect can be neglected. As fluctuations increase with lower space dimensions [15], this gives rise to the definition of critical dimensions:

- Above the upper critical dimension d_c^+ , fluctuations become negligible and the critical exponents take mean-field values.
- Between the upper critical dimension d_c^+ and the lower critical dimension d_c^- , fluctuations become important. The system still undergoes a phase transition, but the mean-field approach fails to deliver valid critical exponents. Here, more sophisticated methods have to be considered like renormalization group techniques [16]. A further discussion of these methods is out of scope of this thesis.
- Below the lower critical dimension d_c^- , fluctuations completely destroy the ordered phase and no phase transition occurs.

2.4 Quantum-to-Classical Correspondence

A powerful concept to study quantum phase transitions is the quantum-to-classical correspondence. With this method, quantum systems in d dimensions can be mapped to classical systems in $d + z$ dimensions, where z is the dynamic critical exponent. Formally, this is done by identifying the density operator $e^{-\hat{H}/k_B T}$ in the partition function $Z = \text{Tr} e^{-\hat{H}/k_B T}$ as a time evolution operator in imaginary time. At zero temperature, this imaginary time direction acts similar to z additional spatial dimensions [12]. This technique will be used later in the context of the Spin-Boson Model to relate its quantum phase transition to the classical transition of a 1D Ising chain with long-ranged interactions.

A more detailed examination of this method can be found in [11].

3 The Spin-Boson Model

The Spin-Boson Model was popularized by Leggett et al. in 1987 in the context of dissipative quantum systems [1] and, since then, has been applied in various contexts [17][18]. In recent years, the focus of interest has been most notably shifted to its widely discussed quantum phase transition at zero temperature [4][5][6][9].

This chapter gives an outline about the static properties of the Spin-Boson Model as well as its quantum critical behaviour.

3.1 The Hamiltonian

The Spin-Boson Model is a simple example of an open quantum system. It describes a two-state system that is coupled to a bath consisting of non-interacting bosons. This leads to the Hamiltonian of the form

$$\hat{H} = -\Delta \frac{\hat{\sigma}_x}{2} + \epsilon \frac{\hat{\sigma}_z}{2} + \sum_i \omega_i \hat{a}_i^\dagger \hat{a}_i + \frac{\hat{\sigma}_z}{2} \sum_i \lambda_i (\hat{a}_i + \hat{a}_i^\dagger). \quad (3.1)$$

The Hamiltonian of any quantum impurity model, like the Spin-Boson Model, consists of three parts: The impurity, which usually has a small number of degrees of freedom, the environment or bath, which can be of bosonic or fermionic nature, and the interaction between impurity and bath. For the Spin-Boson Model, this partition results in the following terms:

$\hat{H}_{TSS} = -\Delta \frac{\hat{\sigma}_x}{2} + \epsilon \frac{\hat{\sigma}_z}{2}$ describes the two-state system; a spin 1/2 impurity, which can be tuned via the tunnelling constant Δ and an additional bias ϵ . Here $\hat{\sigma}_z$ and $\hat{\sigma}_x$ represent the standard Pauli matrices and the reduced Planck constant is set to $\hbar = 1$ throughout the whole thesis.

$\hat{H}_{bath} = \sum_i \omega_i \hat{a}_i^\dagger \hat{a}_i$ represents a non-charged environment, which is characterized by non-interacting harmonic oscillators with frequencies ω_i . The corresponding occupation numbers are given by the operator $\hat{n}_i = \hat{a}_i^\dagger \hat{a}_i$, where \hat{a}_i^\dagger and \hat{a}_i denote the bosonic creation and annihilation operators.

$\hat{H}_{int} = \frac{\hat{\sigma}_z}{2} \sum_i \lambda_i (\hat{a}_i + \hat{a}_i^\dagger)$ characterizes the interaction between spin and environment: the z-component of the spin couples linearly to each oscillator mode i with λ_i specifying the coupling strength.

The effect of the bath can be fully described by the spectral function

$$J(\omega) = \pi \sum_i \lambda_i^2 \delta(\omega - \omega_i), \quad (3.2)$$

which can be interpreted as the bosonic density of states weighted with the coupling strength.

As one is interested in the low energy spectrum of the system, it is convenient to choose a power law form of $J(\omega)$. The standard parametrization is given by

$$J(\omega) = 2\pi\alpha\omega_c^{1-s}\omega^s, \quad 0 < \omega < \omega_c, \quad (3.3)$$

with an upper cutoff frequency ω_c . The dimensionless parameter α describes the coupling strength between the impurity and the bosons, the bath exponent s characterizes the distribution of the bath modes.

One distinguishes three different regions for the bath exponent: the super-ohmic case ($s > 1$), the ohmic case ($s = 1$) and the sub-ohmic case ($s < 1$), each leading to qualitatively different properties of the model (see next section).

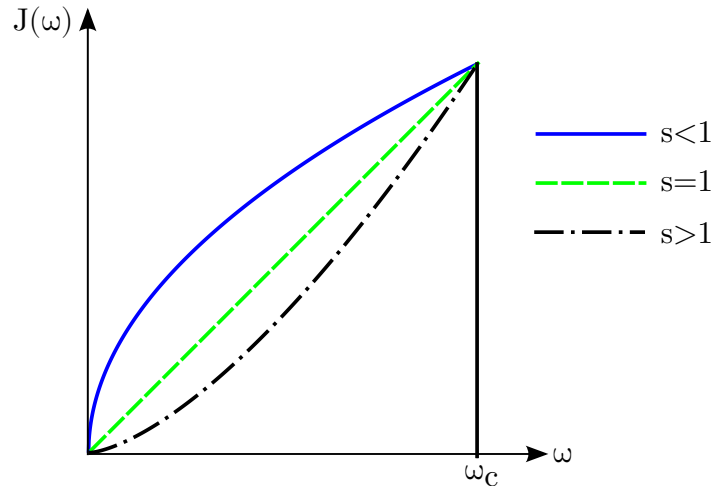


Figure 3.1: Spectral functions for super-ohmic ($s > 1$), ohmic ($s = 1$) and sub-ohmic ($s < 1$) dissipation.

3.2 Critical Behaviour

Setting the bias ϵ to zero, the ground state properties at $T = 0$ are determined only by the tunnelling between the $\hat{\sigma}_z$ -eigenstates given by Δ and the coupling strength to the bosonic bath given by α . This results in two ground state phases that can be distinguished by the order parameter, which in this case is given by the magnetization $\langle \hat{\sigma}_z \rangle$ of the impurity spin:

1. The delocalized phase: the tunnelling between the $\hat{\sigma}_z$ -eigenstates outweighs the coupling in z-direction leading to a weak-coupling phase. The ground state consists of a superposition of $|\uparrow\rangle$ and $|\downarrow\rangle$ at the impurity leading to a vanishing magnetization in coupling direction, i.e. the ground state expectation value $\langle\hat{\sigma}_z\rangle = 0$.
2. The localized phase: in this strong coupling phase, the spin is localized in the direction of the bath coupling. This leads to a two-fold degenerate ground state with finite magnetization, $\langle\hat{\sigma}_z\rangle \neq 0$.

At zero temperature, a quantum phase transition can occur between the localized and the delocalized phase, which is controlled by the coupling parameter α . The character of the transition depends on the bath exponent s . The following cases can be distinguished:

- In the super-ohmic case ($s > 1$) no phase transition occurs: The spin is always delocalized and $\langle\hat{\sigma}_z\rangle = 0$. This can be attributed to the bosonic density of states, which contains only few low energy modes for $s > 1$ leading to a spin-bath interaction that is insufficient to localize the spin.
- In the ohmic case ($s = 1$), both localized and delocalized phase are present and the system undergoes a Kosterlitz-Thouless transition, characterized by an exponentially diverging correlation length for the critical coupling α_c , which depends on the tunnelling parameter Δ and reaches the value $\alpha_c = 1$ in the limit of small Δ [4].
- Considering a sub-ohmic bath spectrum ($s < 1$), the Spin-Boson Model features a second-order quantum phase transition between the localized phase for $\alpha > \alpha_c$ and the delocalized phase for $\alpha < \alpha_c$. This regime has been widely discussed in recent years and will be further examined below.

As described in Chapter 2, a second-order phase transition can be characterized by a set of critical exponents. In this thesis, we focus on the critical exponents β and δ , which in the context of the Spin-Boson Model are defined as follows:

$$\langle\hat{\sigma}_z\rangle \propto (\alpha - \alpha_c)^\beta, \quad (3.4)$$

$$\langle\hat{\sigma}_z\rangle \propto \epsilon^{1/\delta} \text{ at } \alpha = \alpha_c. \quad (3.5)$$

According to quantum-to-classical correspondence (QCC), the sub-ohmic Spin-Boson Model can be mapped on a classical 1D Ising chain with long-range interactions [5]. Thus one can predict the following behaviour for the critical exponents:

- For $s < 1/2$ the system is above its critical dimension and one expects the mean-field values

$$\delta = 3, \quad \beta = 1/2. \quad (3.6)$$

- For $1/2 < s < 1$ the critical exponents have a non-trivial dependency on the bath exponent s . A scaling ansatz for the free energy allows to derive so-called hyperscaling

relations [5]

$$\delta = \frac{1+s}{1-s}, \quad \beta = \nu \frac{1-s}{2}, \quad (3.7)$$

where the correlation length exponent ν is defined by $\xi \propto |\alpha - \alpha_c|^{-\nu}$.

The first numerical results for the sub-ohmic phase transition obtained by the bosonic Numerical Renormalization Group (NRG), however, failed to reproduce these results. Instead hyperscaling was observed for the whole sub-ohmic regime $0 < s < 1$ leading to the conclusion that the QCC failed for the Spin-Boson Model [5]. As discussed in the next chapter, the NRG method is unable to deal with the bosonic nature of the model and therefore its results are not reliable. Supported by other methods confirming the QCC predictions [7] [8], the concept of quantum-to-classical correspondence is now generally considered as validated for the quantum phase transition of the Spin-Boson Model.

3.3 Spin-1-Boson Model

In this thesis, the interest lies in the Spin-Boson Model with spin 1. The examination of this modification is worthwhile as its critical behaviour has not been studied numerically yet, and its treatment will provide useful experience towards more complicated bosonic quantum impurity models featuring spin 1.

The Hamiltonian of the Spin-1-Boson Model is given by

$$\hat{H} = -\Delta \hat{S}_x + \epsilon \hat{S}_z + \sum_i \omega_i \hat{a}_i^\dagger \hat{a}_i + \hat{S}_z \sum_i \lambda_i (\hat{a}_i + \hat{a}_i^\dagger), \quad (3.8)$$

where the spin 1 matrices are given by (see appendix):

$$\hat{S}_x = \frac{1}{\sqrt{2}} \begin{pmatrix} 0 & 1 & 0 \\ 1 & 0 & 1 \\ 0 & 1 & 0 \end{pmatrix} \quad \hat{S}_y = \frac{i}{\sqrt{2}} \begin{pmatrix} 0 & -1 & 0 \\ 1 & 0 & -1 \\ 0 & 1 & 0 \end{pmatrix} \quad \hat{S}_z = \begin{pmatrix} 1 & 0 & 0 \\ 0 & 0 & 0 \\ 0 & 0 & -1 \end{pmatrix} \quad (3.9)$$

in the basis where \hat{S}_z is diagonal.

For the Spin-1-Boson Model one expects the same behaviour of the critical exponents as in the spin 1/2 case, i.e. mean field behaviour for $s < 1/2$ and hyperscaling for $1/2 < s < 1$ [19].

4 Numerical Methods

This chapter reviews the essential numerical methods used to study the Spin-Boson Model. We apply a combination of Wilson's Numerical Renormalization Group (NRG) and the Density Matrix Normalization Group (DMRG) in order to correctly deal with the large bosonic state spaces of the Spin-Boson Model.

Due to the limited scope of this thesis, only the main ideas will be discussed; for a deeper insight see [20][21][22][23].

4.1 Discretization and Mapping of the Hamiltonian

Starting point is the Hamiltonian for the Spin-1-Boson Model defined in the previous chapter

$$\hat{H} = -\Delta\hat{S}_x + \epsilon\hat{S}_z + \sum_i \omega_i \hat{a}_i^\dagger \hat{a}_i + \hat{S}_z \sum_i \lambda_i (\hat{a}_i + \hat{a}_i^\dagger) \quad (4.1)$$

and the spectral function of the bath

$$J(\omega) = 2\pi\alpha\omega_c^{1-s}\omega^s. \quad (4.2)$$

In order to treat the model numerically, a coarse graining has to be applied to the continuous bath spectrum leading to discretized energy levels. Since our study focuses on low energy properties of the model, a logarithmic discretization is chosen, as it yields a finer resolution for small energies than a linear discretization. This results in the following discrete energy levels [20]:

$$\omega_0 = \omega_c \quad (4.3)$$

$$\omega_n = \omega_c \Lambda^{-n}, \quad n = 1, 2, 3, \dots \quad (4.4)$$

where $\Lambda > 1$ is the logarithmic discretization parameter.

The Hamiltonian can now be written in discretized form [21]

$$\hat{H} = -\Delta\hat{S}_x + \epsilon\hat{S}_z + \sum_{n=0}^{\infty} \xi_n \hat{a}_n^\dagger \hat{a}_n + \frac{\hat{S}_z}{\sqrt{\pi}} \sum_{n=0}^{\infty} \gamma_n (\hat{a}_n + \hat{a}_n^\dagger), \quad (4.5)$$

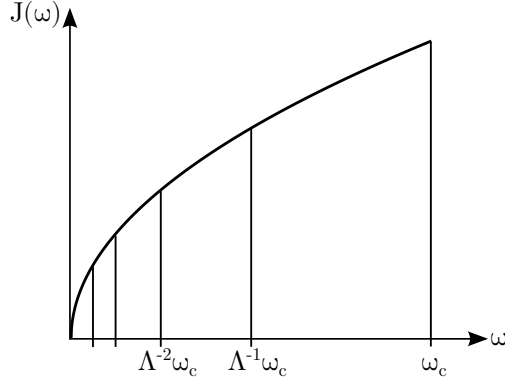


Figure 4.1: Logarithmic discretization of the spectral function (sub-ohmic case).

where

$$\gamma_n^2 = \int_{\Lambda^{-(n+1)}}^{\Lambda^{-n}} J(\omega) d\omega \quad (4.6)$$

$$\xi_n = \gamma_n^{-2} \int_{\Lambda^{-(n+1)}}^{\Lambda^{-n}} J(\omega) \omega d\omega. \quad (4.7)$$

In this form the impurity still couples to each bath mode and the Hamiltonian is therefore referred to as "star"-Hamiltonian [21]. In the next step, the Hamiltonian is mapped to a semi-infinite chain with only nearest-neighbour interaction, the so-called Wilson chain, via a unitary transformation [22]

$$\hat{H} = -\Delta \hat{S}_x + \epsilon \hat{S}_z + \sqrt{\frac{\eta_0}{\pi}} \hat{S}_z (\hat{b}_0 + \hat{b}_0^\dagger) + \sum_{n=0}^{\infty} \epsilon_n \hat{b}_n^\dagger \hat{b}_n + \sum_{n=0}^{\infty} t_n (\hat{b}_n^\dagger \hat{b}_{n+1} + \hat{b}_{n+1}^\dagger \hat{b}_n), \quad (4.8)$$

with the impurity at the first chain site. \hat{b}_n^\dagger and \hat{b}_n are the bosonic creation/annihilation operators for the n-th bosonic site and $\eta_0 = \int J(\omega) d\omega$. The on-site energies ϵ_n and hopping amplitudes t_n decay exponentially with n and have to be calculated numerically [21]. In practice, the semi-infinite chain is approximated by a finite chain of length N .

4.2 NRG Procedure

After transforming the discretized Hamiltonian in the form of 4.8, the model can in principle be solved by using Wilson's Numerical Renormalization Group, which has been successfully applied to fermionic systems in various contexts [3][24]. The NRG procedure is straightforward: One starts with the impurity coupled only to the first bosonic site

$$\hat{H}_0 = -\Delta \hat{S}_x + \epsilon \hat{S}_z + \sqrt{\frac{\eta_0}{\pi}} \hat{S}_z (\hat{b}_0 + \hat{b}_0^\dagger) + \epsilon_0 \hat{b}_0^\dagger \hat{b}_0 \quad (4.9)$$

and then iteratively diagonalizes the Hamiltonian. After obtaining the eigenstates, one adds the next site, rescales the system and repeats the diagonalization procedure. To prevent the exponential growth of the Hilbert space, only a fixed number of eigenstates are kept after each iteration. However, the NRG results obtained in this way disagreed with the predictions from quantum-to-classical correspondence (QCC). The reasons for this failure are discussed below.

4.2.1 Shortcomings of Bosonic NRG

The incorrect NRG results can be attributed to two limitations of bosonic NRG, the Hilbert space truncation and the mass flow error.

- Truncation problem:

In the localized phase, the finite magnetization induces displacements $\hat{x}_i = \frac{1}{\sqrt{2}}(\hat{a}_i + \hat{a}_i^\dagger)$ in the local bosonic state spaces on the Wilson chain. Because of this shift, NRG fails to accurately represent the local state spaces with a truncated basis set. To overcome this problem, a basis of shifted oscillators would be required. Attempts to implement such a basis within the NRG framework failed [21]. However, the VMPS approach, discussed in the following section, is able to cure the bosonic truncation issue.

- Mass-flow error:

The mass-flow error is a direct consequence of the iterative character of the NRG approach. At any iteration step, the system has no information about the rest-chain, i.e. the low-energy modes of the system. This leads to an erroneous modification of the parameters of the system, in particular the coupling strength that controls the quantum phase transition. In consequence, this strongly affects critical exponents obtained from finite size scaling of observables, which are not topic of this thesis. A detailed examination of this issue can be found in [25]. Note that very promising steps have been taken recently to resolve the mass-flow by the usage of an improved construction of the Wilson chain [26].

4.3 VMPS Approach

In this section, the main ideas of VMPS (Variational Matrix Product State) and its application to the Spin-Boson Model will be discussed. VMPS is mathematically equivalent to the Density Matrix Renormalization Group (DMRG) [27] and can be seen as a more intuitive approach. Furthermore, its underlying structure, the matrix product states (MPS), can be also used as the basis for NRG [28] leading to an interesting connection between the two methods.

4.3.1 Matrix Product States

Matrix product states are an elegant way to represent quantum states. A general quantum state of a 1D system with open boundary conditions

$$|\Psi\rangle = \sum_{\sigma_1, \dots, \sigma_N} c_{\sigma_1, \dots, \sigma_N} |\sigma_1, \dots, \sigma_N\rangle \quad (4.10)$$

can be written in MPS language as

$$|\Psi\rangle = \sum_{\sigma_1, \dots, \sigma_N} A^{[\sigma_1]} \dots A^{[\sigma_N]} |\sigma_1, \dots, \sigma_N\rangle \quad (4.11)$$

by decomposing the coefficients $c_{\sigma_1, \dots, \sigma_N}$ into a set of matrices $A^{[\sigma_i]}$. Each tensor $A^{[\sigma_i]}$ connects to a state space $\{|\sigma_i\rangle\}$ of dimension d at site i .

To keep a numerical treatment feasible, the dimension D of $A^{[\sigma_i]}$ must be restricted and a truncation scheme has to be applied. In DMRG, this is accomplished by keeping only the D states with the highest eigenvalues of the density matrix of the currently considered sub-space of the system. A criteria for the efficiency of this truncation method is the rate of decrease of eigenvalues, which is related to the entanglement of the system given by the von Neumann entropy S .

It is found, that for the ground state the entropy scales as the surface of the subregion and not as its volume [29], as one would expect for the entropy as an extensive property in thermodynamics. This "area law" yields an entanglement of the ground state that is constant for one dimensional systems and growing with system size for higher dimensions. Therefore, DMRG is very efficient for one dimensional systems, but its usage is very restricted in the case of higher dimensional systems.

A detailed review of matrix product states in connection with DMRG can be found in [23].

4.3.2 Variational Optimization

The goal of the VMPS approach is to variationally find an approximation for the ground state of the system, i.e. the state that minimizes the energy $E = \frac{\langle \Psi | \hat{H} | \Psi \rangle}{\langle \Psi | \Psi \rangle}$. To achieve this, one starts with a randomly generated MPS of the form 4.11 and then optimizes the A matrices

$$\frac{\partial}{\partial A^i} \frac{\langle \Psi | \hat{H} | \Psi \rangle}{\langle \Psi | \Psi \rangle} = 0 \quad (4.12)$$

one at a time, beginning with the first bosonic site and working through the Wilson chain towards the low energy sites (this procedure is called a DMRG sweep). This process is repeated until convergence is reached, i.e. the approximated ground state energy does not change any further within the desired precision.

4.3.3 Capture of the Bosonic Shifts

As already mentioned, the problem with the bosonic displacements in the localized phase can be treated with a basis of shifted oscillators in the VMPS approach. In [9] this was accomplished during the optimization process: The displacements $\langle \hat{x}_k \rangle$ of the current variational state are used to construct the basis for the next variational state, which is directly incorporated in the Hamiltonian by using shifted bosonic operators $\tilde{b}_k = \hat{b}_k - \frac{1}{\sqrt{2}} \langle \hat{x}_k \rangle$.

In this thesis another method is used. We follow the proposal of [30], where the shift is calculated analytically. The Hamiltonian (4.8) is written in terms of shifted operators $\tilde{b}_i^\dagger = \hat{b}_i^\dagger + \frac{1}{\sqrt{2}} \delta_i$, $\tilde{b}_i = \hat{b}_i + \frac{1}{\sqrt{2}} \delta_i$, resulting in the form

$$\begin{aligned} \hat{H} = & -\Delta \hat{S}_x + \epsilon \hat{S}_z + 2\sqrt{\frac{\eta_0}{\pi}} \hat{S}_z (\tilde{b}_0 + \tilde{b}_0^\dagger) - 2\sqrt{2} \delta_0 \eta_0 \hat{S}_z \\ & + \sum_{n=0}^{\infty} \epsilon_n (\tilde{b}_n^\dagger \tilde{b}_n - \frac{1}{\sqrt{2}} \delta_n (\tilde{b}_n + \tilde{b}_n^\dagger) + \frac{1}{2} \delta_n^2) \\ & + \sum_{n=0}^{\infty} t_n (\tilde{b}_n^\dagger \tilde{b}_{n+1} + \tilde{b}_{n+1}^\dagger \tilde{b}_n - \frac{1}{\sqrt{2}} \delta_{n+1} (\tilde{b}_n + \tilde{b}_n^\dagger) - \frac{1}{\sqrt{2}} \delta_n (\tilde{b}_{n+1} + \tilde{b}_{n+1}^\dagger) + \delta_n \delta_{n+1}). \end{aligned} \quad (4.13)$$

In the optimized basis the bosonic displacements are minimized, hence all terms containing $(\tilde{b}_n + \tilde{b}_n^\dagger)$ in the Hamiltonian must vanish. By replacing \hat{S}_z by its mean value, one can derive equations for the δ_n that fulfil this condition (see [30] for details).

For δ_0 one obtains a continued fraction

$$\delta_0 = \frac{-2\sqrt{2\eta_0/\pi} \langle \hat{S}_z \rangle}{\epsilon_0 - \frac{t_0^2}{\epsilon_1 - \frac{t_1^2}{\ddots}}} \quad (4.14)$$

and the other δ_n can be calculated recursively via

$$\delta_n = -\delta_{n-1} \frac{t_{n-1}^2}{\epsilon_n - \frac{t_n^2}{\epsilon_{n+1} - \frac{t_{n+1}^2}{\ddots}}} \quad (4.15)$$

In this optimized basis the system undergoes one optimization sweep (this is in contrast to the method discussed above, where the shifts are recalculated at each sweeping step). Afterwards, the displacements are recalculated for the next sweep and the process is iterated until convergence is reached.

5 Results

This chapter presents the results for the Spin-1-Boson Model that are obtained using the VMPS method. The aim is to create the sub-ohmic phase diagram as well as to determine the values for the critical exponents β and δ . For all results the following parameters are used:

Description	Parameter	Value
chain length	N	50
discretization parameter	Λ	2
tunnelling amplitude	Δ	0.1
bond dimension	D	40
local state space dimension	d_k	100
OBB dimension	d_{opt}	12

Table 5.1: Parameters used for the study of the Spin-1-Boson Model. The bond dimension of the A tensors is given by D and d_k denotes the dimension of the bosonic sites. The local states are represented in an optimized boson basis (OBB) of dimension d_{opt} , see [9][20] for details.

5.1 Phase Boundary

In order to study the critical properties of the model, it is necessary to find the critical coupling strength α_c for a given set of parameters. The phase boundary is obtained by using a bisection method: One starts with an interval $[\alpha_1, \alpha'_1]$ large enough to contain the critical coupling strength with certainty, i.e. the coupling strength $\alpha = \alpha_1$ leads to the delocalized phase and $\alpha = \alpha'_1$ to the localized phase. Then a VMPS run is performed for the coupling strength $\alpha = \frac{1}{2}(\alpha_1 + \alpha'_1)$. By checking whether or not this coupling leads to localization, one can narrow down the interval that contains the critical coupling α_c . This process is iterated until the desired precision is reached (the results in this thesis have a precision of 10^{-8}).

Essential for this method is a reliable way to determine in which phase the system is located. In this thesis, this is achieved by examining the occupation numbers of the bosonic sites. In the delocalized phase, the occupation numbers n_k for the k -th bosonic sites decrease with increasing k , whereas they diverge in the localized phase [21] (see Figure 5.1).

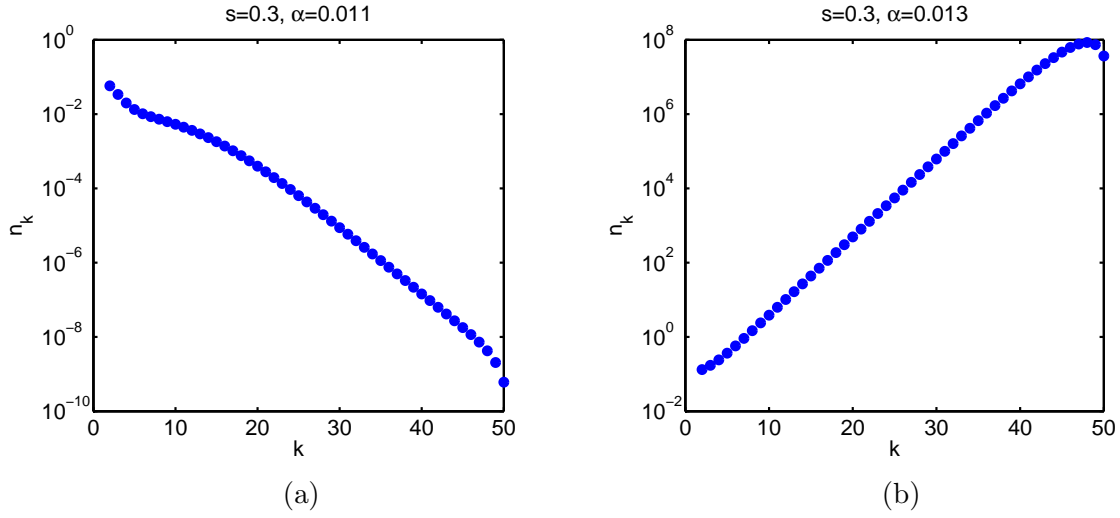


Figure 5.1: Bosonic occupation numbers for the delocalized phase (a) and the localized phase (b). The bosonic displacements in the localized phase lead to a divergence of the occupation numbers towards the end of the chain.

With this method, the critical couplings for different values of s can be determined. The resulting phase diagram and the calculated values are shown in Figure 5.2. One can observe a critical coupling strength decreasing with smaller values of the bath exponent s . This behaviour is expected and analog to the spin 1/2 model, since the number of bath oscillators at low energies that are responsible for the localization of the impurity spin increases strongly with decreasing s .

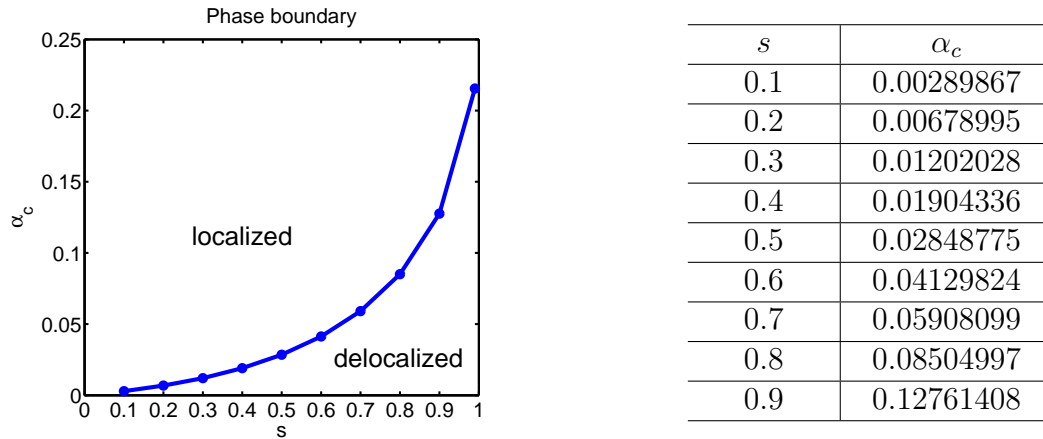
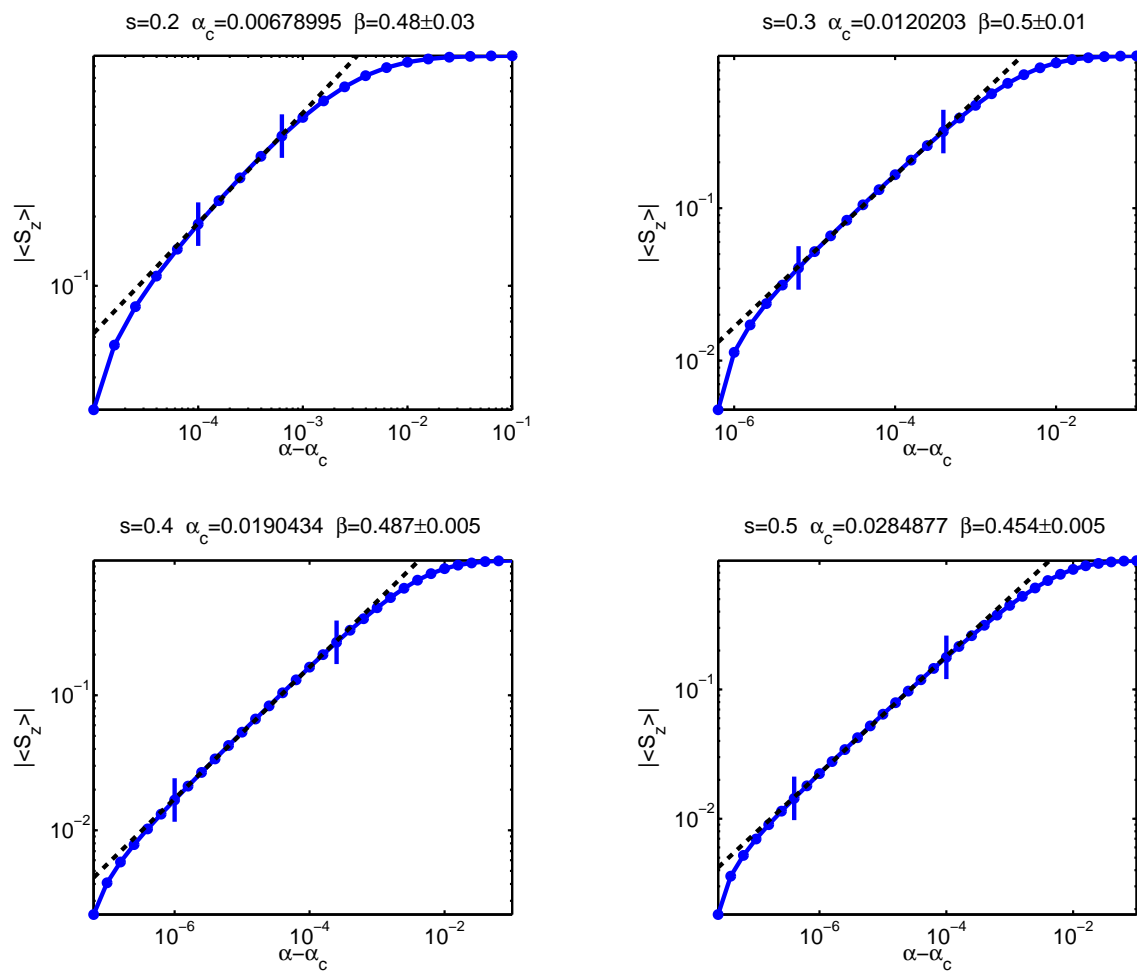


Figure 5.2: Sub-ohmic phase diagram and values for the critical coupling. The critical coupling strength α_c decreases with smaller values of s .

5.2 Critical Exponents

This section describes how the behaviour of the critical exponents β and δ under variation of the bath exponent s are examined and presents the results.

As discussed in Chapter 3, one expects a power-law behaviour for the magnetization $\langle \hat{S}_z \rangle$ in the vicinity of the critical coupling α_c , $\langle \hat{S}_z \rangle \propto (\alpha - \alpha_c)^\beta$ with the bias set to $\epsilon = 0$. By measuring the magnetization for different values of $(\alpha - \alpha_c)$, one would expect a straight line on a double-logarithmic plot. The value of β can then be extracted from the slope of this line.



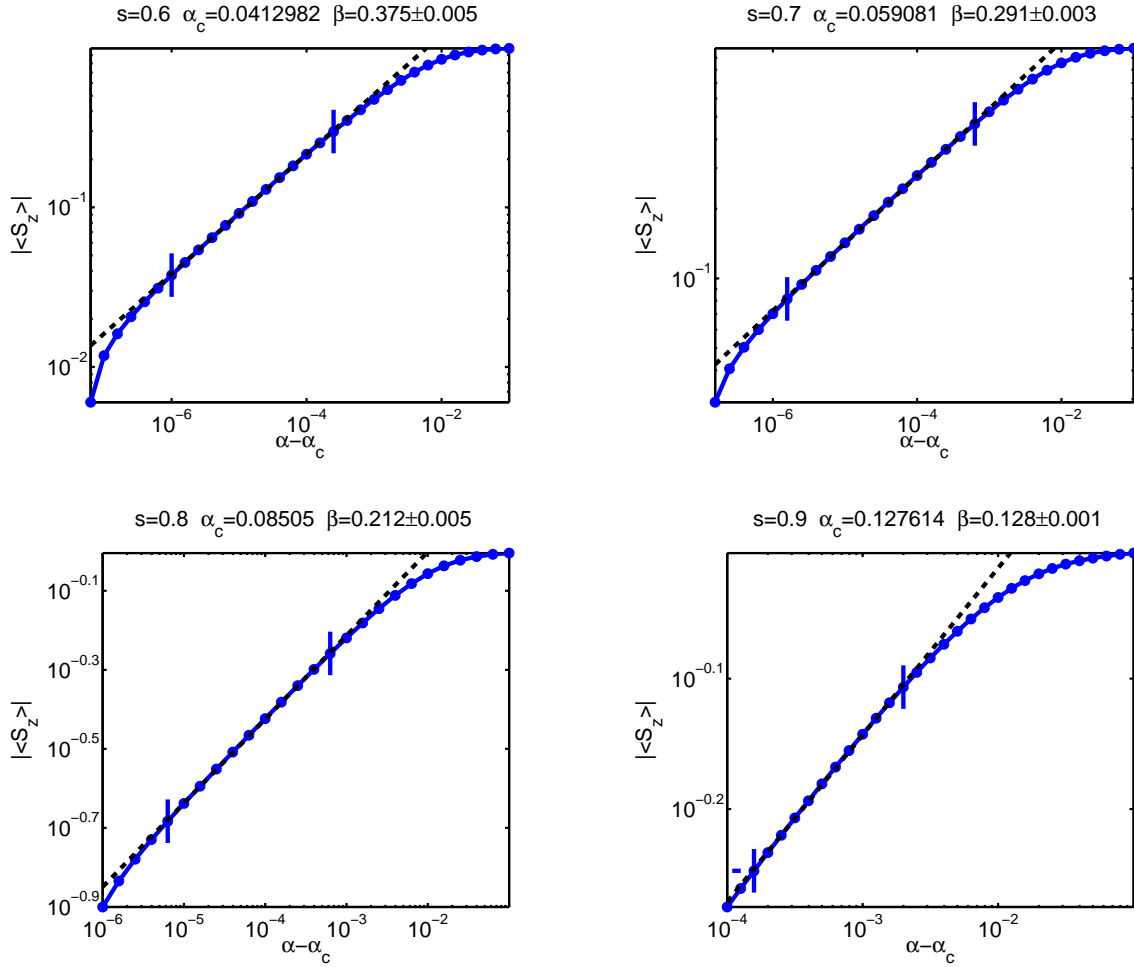


Figure 5.3: VMPS results for the magnetization $|\langle \hat{S}_z \rangle|$ close to the phase boundary (blue dotted lines) for various values of s . The dashed black lines indicate the power-law fits used to extract the critical exponent β . The vertical lines illustrate the fitting intervals.

Figure 5.3 displays the numerical results used to extract β for a variety of s -values. In all panels, we observe a solid power-law scaling over several decades that allows to extract β with high precision. The approximated fitting error is estimated by varying the fitting intervals and observing the effect on the value of the critical exponent β .

Note that the range of power-law scaling for $s = 0.2$ is shorter than for larger values of s . The reason for this behaviour is that the chain length needed to determine α_c within a desired precision scales with the correlation length exponent ν [20], which is found to diverge for $s \rightarrow 0$ [4]. The case $s = 0.1$ is omitted in this thesis, as the scaling range is too small to produce suitable data for the critical exponents.

Using these results, one can now examine the s -dependence of β . As discussed in Chapter 3, quantum-to-classical correspondence predicts mean-field values for $s < 1/2$ and hyperscaling for $1/2 < s < 1$. Figure 5.4 shows the resulting values of $1/\beta$ against s .

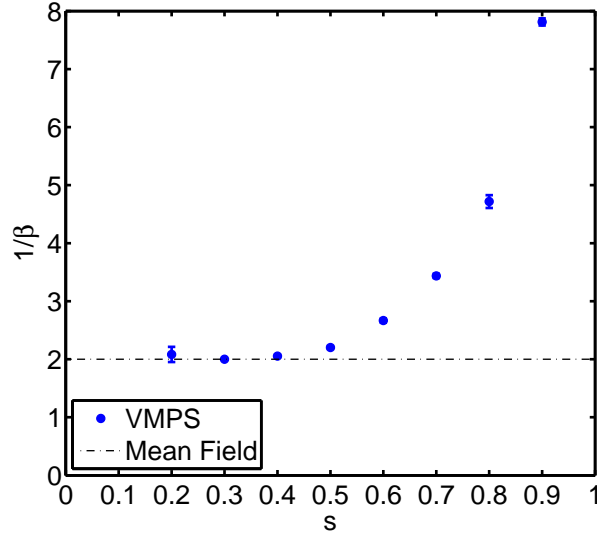
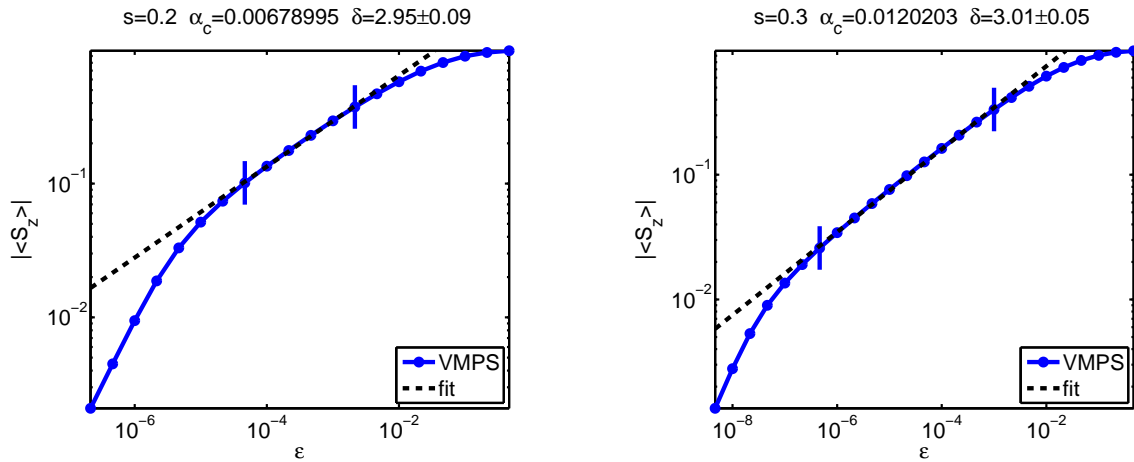


Figure 5.4: s -dependence of the critical exponent β . The from Figure 5.3 collected VMPS results for β clearly follow the mean-field prediction $1/\beta = 2$ for $s < 1/2$ (black dashed line).

As expected [19], β is found to take the mean-field value $\beta = 1/2$ for $s < 1/2$ and shows an s -dependent behaviour for $s > 1/2$, indicating hyperscaling. At $s = 1/2$, the value of β slightly deviates from its mean-field value. This can be attributed to logarithmic corrections to mean-field behaviour that occur when the model is at its upper critical dimension [15].

The critical exponent δ , defined via $\langle \hat{S}_z \rangle \propto \epsilon^{1/\delta}$ at the critical coupling $\alpha = \alpha_c$, is evaluated in a similar fashion. For each value of s , the magnetization is plotted under variation of ϵ for $\alpha = \alpha_c$. The VMPS results for δ are illustrated in Figure 5.5.



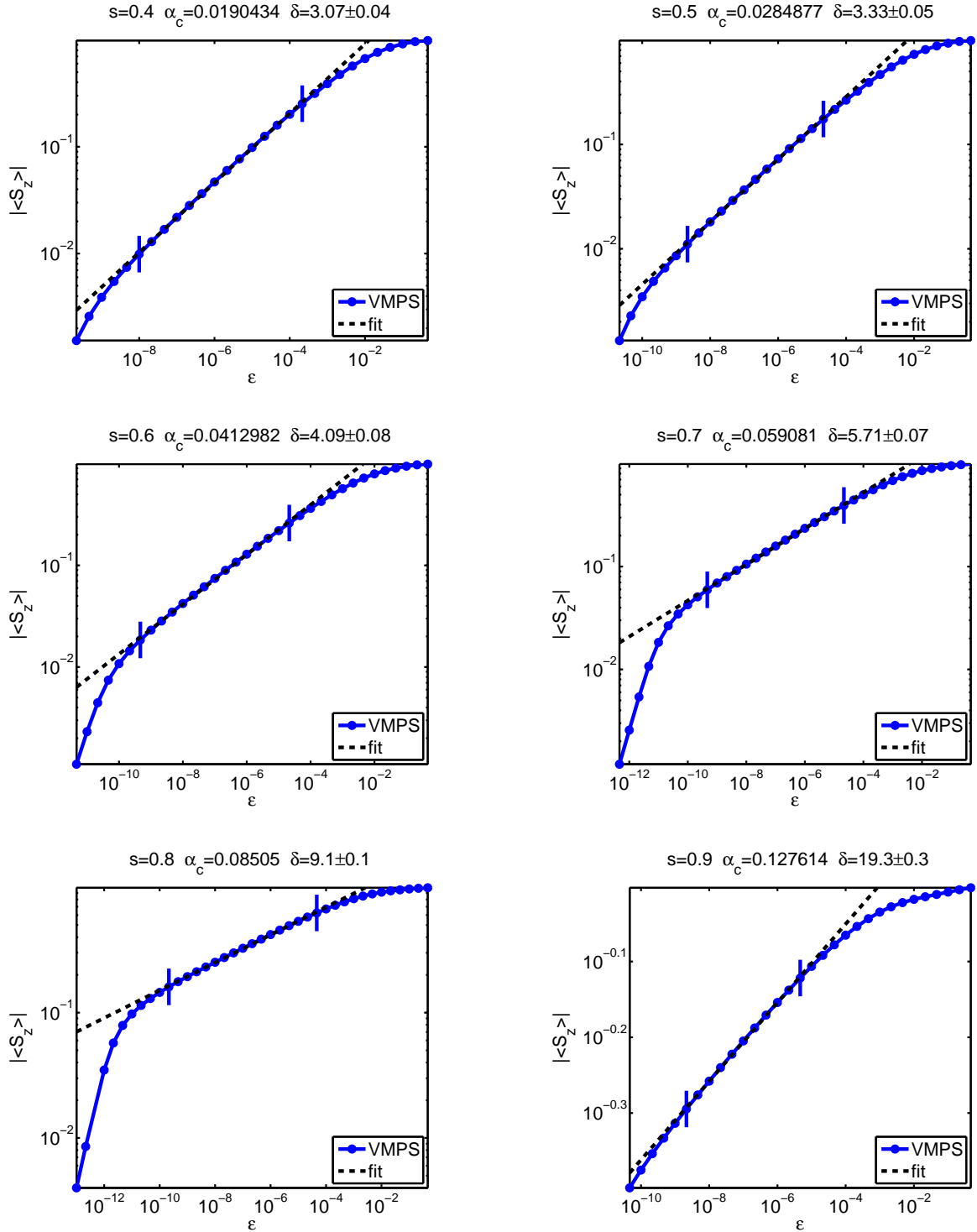


Figure 5.5: VMPS results for the magnetization $|\langle \hat{S}_z \rangle|$ at the critical point in response to an external field ϵ for various values of s (blue dotted lines). Characteristic power-law scaling of $|\langle \hat{S}_z \rangle|$ is used to extract the critical exponent δ via fitting (black dashed line). The vertical lines indicate the fitting intervals.

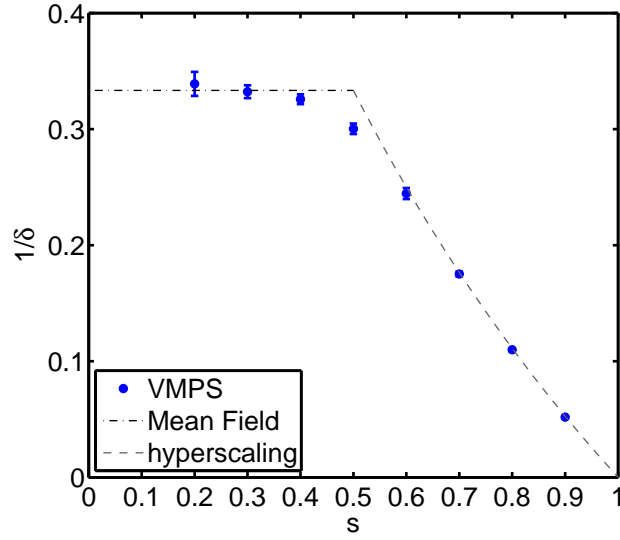


Figure 5.6: s -dependence of the critical exponent δ . The from Figure 5.5 collected VMPS results for δ clearly follow the mean-field predictions $1/\delta = 1/3$ for $s < 1/2$ (black dashed line) and are in agreement with hyperscaling for $s > 1/2$ (grey dashed line).

As for the critical exponent β , solid power-law scaling allows to extract δ from the scaling behaviour of $\langle \hat{S}_z \rangle$. Again one can observe a comparatively short range of power-law scaling for $s = 0.2$ with the same reason as discussed above.

The behaviour of the critical exponent δ is also consistent with the theoretical predictions, as shown in Figure 5.6. For $s < 1/2$, mean-field values are obtained with logarithmic corrections at the upper critical dimension $s = 1/2$. For $s > 1/2$, δ shows excellent agreement with the hyperscaling result $\delta = \frac{1+s}{1-s}$.

Considering these results for the critical exponents β and δ , one can conclude that the quantum-to-classical correspondence holds for the Spin-1-Boson Model.

6 Conclusion

In this thesis, we studied the critical behaviour of the Spin-1-Boson Model. In Chapter 2, we reviewed the essential physical aspects of phase transitions. After a short summary of the basic features of classical and quantum phase transitions, we motivated the definition of critical exponents. We proceeded by giving an overview of mean-field theories and quantum-to-classical correspondence, which both are important concepts for the treatment of critical behaviour.

In Chapter 3, we discussed the Spin-Boson Model. After summarizing the basic properties, we examined the critical properties of the model. There, we focussed on the sub-ohmic quantum phase transition and made predictions for the dependence of the critical exponents β and δ on the bath exponent s .

In Chapter 4, we gave an outline on the numerical methods that are important for the Spin-Boson Model. After discretizing the Hamiltonian and mapping it on the Wilson chain, we reviewed the NRG method and revealed its limitations in the application on bosonic systems. We resumed by introducing the VMPS method and its ability to overcome the problems of bosonic NRG.

In Chapter 5, we presented our results for the Spin-1-Boson Model obtained by the VMPS method. We obtained the sub-ohmic phase diagram, which we found to have the same qualitative features as for the spin 1/2 case. Subsequently we extracted the critical exponents β and δ and examined their s -dependence. The results were consistent with the theoretical predictions and we therefore concluded the validity of the quantum-to-classical correspondence for the Spin-1-Boson Model.

This thesis proved the capability of the VMPS method to deal with spin-1 impurities. As an outlook, one could therefore proceed by studying further spin-1 impurity models with VMPS. An example would be the Spin-Boson Model with two baths. For this system, an examination of the spin 1/2 case yielded comprehensive results with a rich phase diagram [9][20]. However, early data for the spin 1 case turned out to be contradictory. As the VMPS method generally seems to be convenient also for spin 1 impurities, a further study of this model with VMPS should be worthwhile.

7 Appendix

7.1 Derivation of the Spin-1 Matrices

A general spin state in the z-basis can be written as $|S, m\rangle$, where S denotes the total spin and m the projection on the z-axis. In our case $S = 1$; therefore we use the notations

$$|\uparrow\rangle = |1, 1\rangle, \quad |\rightarrow\rangle = |1, 0\rangle, \quad |\downarrow\rangle = |1, -1\rangle. \quad (7.1)$$

These states are orthonormal and fulfil the eigenvalue equations ($\hbar = 1$)

$$\hat{S}_z |\uparrow\rangle = +1 |\uparrow\rangle \quad (7.2)$$

$$\hat{S}_z |\rightarrow\rangle = 0 |\rightarrow\rangle \quad (7.3)$$

$$\hat{S}_z |\downarrow\rangle = -1 |\downarrow\rangle. \quad (7.4)$$

Therefore the matrix representation of \hat{S}_z in the z-basis is given by

$$\hat{S}_z = \begin{pmatrix} \langle\uparrow|\hat{S}_z|\uparrow\rangle & \langle\uparrow|\hat{S}_z|\rightarrow\rangle & \langle\uparrow|\hat{S}_z|\downarrow\rangle \\ \langle\rightarrow|\hat{S}_z|\uparrow\rangle & \langle\rightarrow|\hat{S}_z|\rightarrow\rangle & \langle\rightarrow|\hat{S}_z|\downarrow\rangle \\ \langle\downarrow|\hat{S}_z|\uparrow\rangle & \langle\downarrow|\hat{S}_z|\rightarrow\rangle & \langle\downarrow|\hat{S}_z|\downarrow\rangle \end{pmatrix} = \begin{pmatrix} 1 & 0 & 0 \\ 0 & 0 & 0 \\ 0 & 0 & -1 \end{pmatrix}. \quad (7.5)$$

To calculate the matrix representations of \hat{S}_x and \hat{S}_y , one needs the raising and lowering operators \hat{S}_+ and \hat{S}_- , defined via $\hat{S}_\pm = \hat{S}_x \pm i\hat{S}_y$. These fulfil the relation

$$\hat{S}_\pm |S, m\rangle = \sqrt{S(S+1) - m(m \pm 1)} |S, m \pm 1\rangle. \quad (7.6)$$

For $S=1$ this yields

$$\hat{S}_+ |\uparrow\rangle = 0, \quad \hat{S}_+ |\rightarrow\rangle = \sqrt{2} |\uparrow\rangle, \quad \hat{S}_+ |\downarrow\rangle = \sqrt{2} |\rightarrow\rangle \quad (7.7)$$

$$\hat{S}_- |\uparrow\rangle = \sqrt{2} |\rightarrow\rangle, \quad \hat{S}_- |\rightarrow\rangle = \sqrt{2} |\downarrow\rangle, \quad \hat{S}_- |\downarrow\rangle = 0, \quad (7.8)$$

leading to the matrix representations

$$\hat{S}_+ = \begin{pmatrix} \langle\uparrow|\hat{S}_+|\uparrow\rangle & \langle\uparrow|\hat{S}_+|\rightarrow\rangle & \langle\uparrow|\hat{S}_+|\downarrow\rangle \\ \langle\rightarrow|\hat{S}_+|\uparrow\rangle & \langle\rightarrow|\hat{S}_+|\rightarrow\rangle & \langle\rightarrow|\hat{S}_+|\downarrow\rangle \\ \langle\downarrow|\hat{S}_+|\uparrow\rangle & \langle\downarrow|\hat{S}_+|\rightarrow\rangle & \langle\downarrow|\hat{S}_+|\downarrow\rangle \end{pmatrix} = \begin{pmatrix} 0 & \sqrt{2} & 0 \\ 0 & 0 & \sqrt{2} \\ 0 & 0 & 0 \end{pmatrix}, \quad (7.9)$$

$$\hat{S}_- = \begin{pmatrix} \langle \uparrow | \hat{S}_- | \uparrow \rangle & \langle \uparrow | \hat{S}_- | \rightarrow \rangle & \langle \uparrow | \hat{S}_- | \downarrow \rangle \\ \langle \rightarrow | \hat{S}_- | \uparrow \rangle & \langle \rightarrow | \hat{S}_- | \rightarrow \rangle & \langle \rightarrow | \hat{S}_- | \downarrow \rangle \\ \langle \downarrow | \hat{S}_- | \uparrow \rangle & \langle \downarrow | \hat{S}_- | \rightarrow \rangle & \langle \downarrow | \hat{S}_- | \downarrow \rangle \end{pmatrix} = \begin{pmatrix} 0 & 0 & 0 \\ \sqrt{2} & 0 & 0 \\ 0 & \sqrt{2} & 0 \end{pmatrix}. \quad (7.10)$$

The matrix representations of \hat{S}_x and \hat{S}_y can now be calculated via

$$\hat{S}_x = \frac{1}{2}(\hat{S}_+ + \hat{S}_-) \quad (7.11)$$

$$\hat{S}_y = \frac{1}{2i}(\hat{S}_+ - \hat{S}_-) \quad (7.12)$$

leading to the results

$$\hat{S}_x = \frac{1}{\sqrt{2}} \begin{pmatrix} 0 & 1 & 0 \\ 1 & 0 & 1 \\ 0 & 1 & 0 \end{pmatrix} \quad \hat{S}_y = \frac{i}{\sqrt{2}} \begin{pmatrix} 0 & -1 & 0 \\ 1 & 0 & -1 \\ 0 & 1 & 0 \end{pmatrix}. \quad (7.13)$$

Bibliography

- [1] A. J. Leggett et al., “Dynamics of the dissipative two-state system”, *Rev. Mod. Phys.* **59**, 1 (1987).
- [2] K. G. Wilson, “Renormalization group and critical phenomena. I. Renormalization group and the Kadanoff scaling picture”, *Phys. Rev. B* **4**, 3141 (1971).
- [3] K. G. Wilson, “The renormalization group: Critical phenomena and the Kondo problem”, *Rev. Mod. Phys.* **47**, 773 (1975).
- [4] R. Bulla, N.-H. Tong, and M. Vojta, “Numerical renormalization group for bosonic systems and application to the sub-ohmic spin-boson model”, *Phys. Rev. Lett.* **91**, 170601 (2003).
- [5] M. Vojta, N.-H. Tong, and R. Bulla, “Quantum phase transitions in the sub-ohmic spin-boson model: Failure of the quantum-classical mapping”, *Phys. Rev. Lett.* **94**, 070604 (2005).
- [6] M. Vojta, N.-H. Tong, and R. Bulla, “Erratum: Quantum phase transitions in the sub-ohmic spin-boson model: Failure of the quantum-classical mapping [*Phys. Rev. Lett.* 94, 070604 (2005)]”, *Phys. Rev. Lett.* **102**, 249904 (2009).
- [7] A. Winter, H. Rieger, M. Vojta, and R. Bulla, “quantum phase transition in the sub-ohmic spin-boson model: Quantum Monte Carlo study with a continuous imaginary time cluster algorithm”, *Phys. Rev. Lett.* **102**, 030601 (2009).
- [8] A. Alvermann and H. Fehske, “Sparse polynomial space approach to dissipative quantum systems: Application to the sub-ohmic spin-boson model”, *Phys. Rev. Lett.* **102**, 150601 (2009).
- [9] C. Guo, A. Weichselbaum, J. von Delft, and M. Vojta, “Critical and strong-coupling phases in one- and two-bath spin-boson models”, *Phys. Rev. Lett.* **108**, 160401 (2012).
- [10] T. Vojta, “Computing quantum phase transitions”, *Reviews in Computational Chemistry* **26**, 167 (2008).
- [11] S. Sachdev, *Quantum Phase Transitions*, Cambridge University Press (2001).
- [12] M. Vojta, “Quantum phase transitions”, *Reports on Progress in Physics* **66**, 2069 (2003).

-
- [13] Y.-P. Shim, S. Oh, J. Fei, X. Hu, and M. Friesen, “Probing quantum phase transitions in a spin chain with a double quantum dot”, *Phys. Rev. B* **87**, 155405 (2013).
- [14] R. Schneider, A. G. Zaitsev, D. Fuchs, and H. v. Lhneysen, “Superconductor-insulator quantum phase transition in disordered FeSe thin films”, *Phys. Rev. Lett.* **108**, 257003 (2012).
- [15] J. Als-Nielsen and R. Birgeneau, “Mean field theory, the Ginzburg criterion, and marginal dimensionality of phase transitions”, *American Journal of Physics* **45**, 554 (1977).
- [16] A. Pelissetto and E. Vicari, “Critical phenomena and renormalization-group theory”, *Physics Reports* **368**, 549 (2002).
- [17] A. Recati, P. O. Fedichev, W. Zwerger, J. von Delft, and P. Zoller, “Atomic quantum dots coupled to a reservoir of a superfluid bose-einstein condensate”, *Phys. Rev. Lett.* **94**, 040404 (2005).
- [18] D. Porras, F. Marquardt, J. von Delft, and J. I. Cirac, “Mesoscopic spin-boson models of trapped ions”, *Phys. Rev. A* **78**, 010101 (2008).
- [19] M. Vojta, private communication (2014).
- [20] C. Guo, A. Weichselbaum, J. von Delft, and M. Vojta, “Supplementary information for ‘critical and strong-coupling phases in one- and two-bath spin-boson models’”, *Phys. Rev. Lett.* **108**, 160401 (2012).
- [21] R. Bulla, H.-J. Lee, N.-H. Tong, and M. Vojta, “Numerical renormalization group for quantum impurities in a bosonic bath”, *Phys. Rev. B* **71**, 045122 (2005).
- [22] C. Guo, *Using Density Matrix Renormalization Group to Study Open Quantum Systems*, Ph.D. thesis, Ludwig-Maximilians-University Munich (2012).
- [23] U. Schollwöck, “The density-matrix renormalization group in the age of matrix product states”, *Annals of Physics* **326**, 1, 96–192 (2011).
- [24] R. Bulla, T. A. Costi, and T. Pruschke, “Numerical renormalization group method for quantum impurity systems”, *Rev. Mod. Phys.* **80**, 395 (2008).
- [25] M. Vojta, R. Bulla, F. Güttge, and F. Anders, “Mass-flow error in the numerical renormalization-group method and the critical behavior of the sub-Ohmic spin-boson model”, *Phys. Rev. B* **81**, 075122 (2010).
- [26] N. Linden et al., to be published.
- [27] S. Ostlund and S. Rommer, “Thermodynamic limit of density matrix renormalization”, *Phys. Rev. Lett.* **75**, 3537 (1995).

-
- [28] A. Weichselbaum, F. Verstraete, U. Schollwöck, J. I. Cirac, and J. von Delft, “Variational matrix-product-state approach to quantum impurity models”, *Phys. Rev. B* **80**, 165117 (2009).
- [29] J. Eisert, M. Cramer, and M. B. Plenio, “Colloquium: Area laws for the entanglement entropy”, *Rev. Mod. Phys.* **82**, 277 (2010).
- [30] F. Güttge, *Real-Time Dynamics and Critical Phenomena of Quantum Impurity Systems*, Ph.D. thesis, Technical University of Dortmund (2012).

Selbstständigkeitserklärung

Hiermit erkläre ich, dass ich die vorliegende Arbeit selbstständig verfasst und keine anderen als die angegebenen Quellen und Hilfsmittel benutzt habe.

München, 30. Juni 2014

Ort, Datum

Manuel Lindner